

Clinical Article



# Deep Learning-Based Localization and Orientation Estimation of Pedicle Screws in Spinal Fusion Surgery

Kwang Hyeon Kim <sup>1</sup>, Hae-Won Koo <sup>2</sup>, and Byung-Jou Lee <sup>2</sup>

<sup>1</sup>Clinical Research Support Center, Inje University Ilsan Paik Hospital, Goyang, Korea

<sup>2</sup>Department of Neurosurgery, Inje University Ilsan Paik Hospital, Inje University College of Medicine, Goyang, Korea



Received: Mar 25, 2024

Revised: Jun 3, 2024

Accepted: Jun 4, 2024

Published online: Jun 17, 2024

Address for correspondence:

Byung-Jou Lee

Department of Neurosurgery, Inje University Ilsan Paik Hospital, Inje University College of Medicine, 170 Juhwa-ro, Ilsanseo-gu, Goyang 10380, Korea.

Email: lbjguri@hanmail.net

Copyright © 2024 Korean Neurotraumatology Society

This is an Open Access article distributed under the terms of the Creative Commons Attribution Non-Commercial License (<https://creativecommons.org/licenses/by-nc/4.0/>) which permits unrestricted non-commercial use, distribution, and reproduction in any medium, provided the original work is properly cited.

## ORCID iDs

Kwang Hyeon Kim

<https://orcid.org/0000-0003-0434-1905>

Hae-Won Koo

<https://orcid.org/0000-0001-7014-3005>

Byung-Jou Lee

<https://orcid.org/0000-0002-4030-3618>

## ABSTRACT

**Objective:** This study investigated the application of a deep learning-based object detection model for accurate localization and orientation estimation of spinal fixation surgical instruments during surgery.

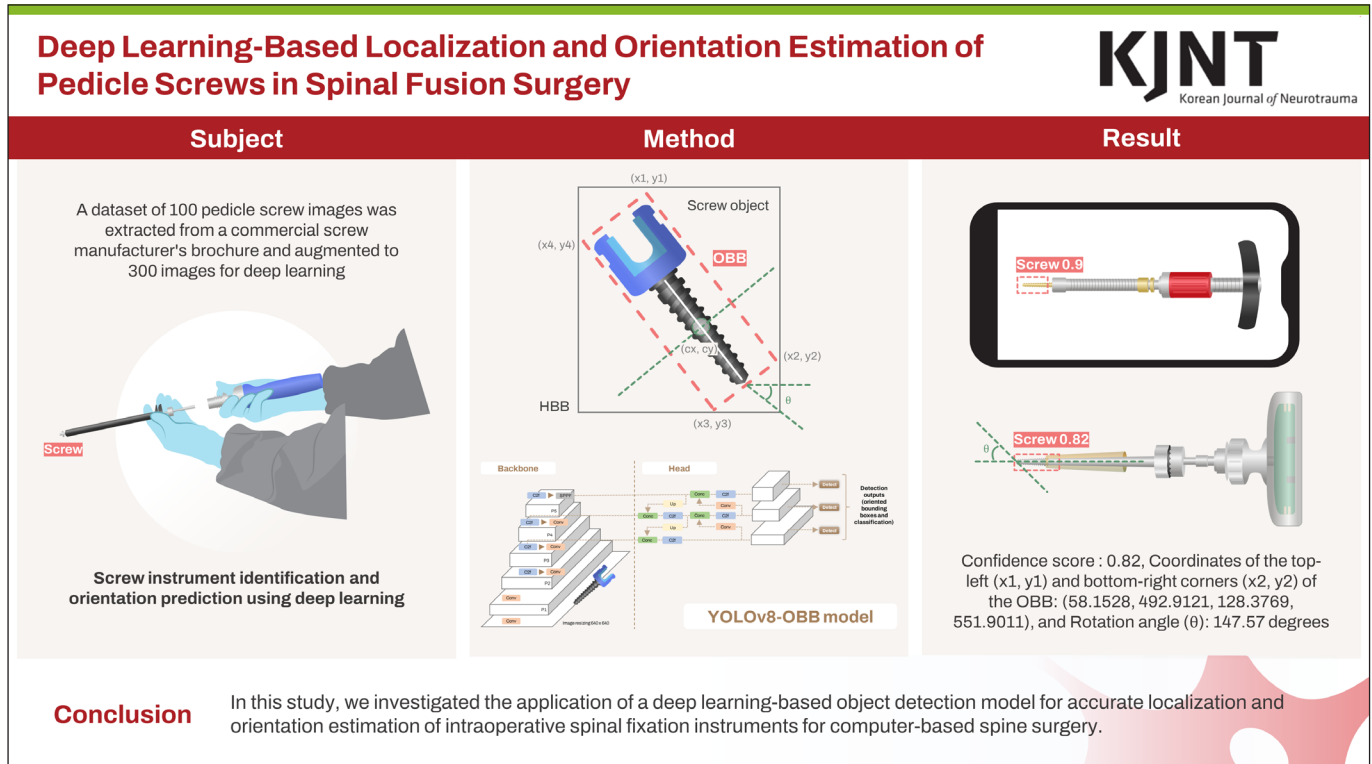
**Methods:** We employed the You Only Look Once (YOLO) object detection framework with oriented bounding boxes (OBBs) to address the challenge of non-axis-aligned instruments in surgical scenes. The initial dataset of 100 images was created using brochure and website images from 11 manufacturers of commercially available pedicle screws used in spinal fusion surgeries, and data augmentation was used to expand 300 images. The model was trained, validated, and tested using 70%, 20%, and 10% of the images of lumbar pedicle screws, with the training process running for 100 epochs.

**Results:** The model testing results showed that it could detect the locations of the pedicle screws in the surgical scene as well as their direction angles through the OBBs. The F1 score of the model was 0.86 (precision: 1.00, recall: 0.80) at each confidence level and mAP50. The high precision suggests that the model effectively identifies true positive instrument detections, although the recall indicates a slight limitation in capturing all instruments present. This approach offers advantages over traditional object detection in bounding boxes for tasks where object orientation is crucial, and our findings suggest the potential of YOLOv8 OBB models in real-world surgical applications such as instrument tracking and surgical navigation.

**Conclusion:** Future work will explore incorporating additional data and the potential of hyperparameter optimization to improve overall model performance.

**Keywords:** Pedicle screw; Deep learning; Spine; Surgical instruments; Localization

## GRAPHICAL ABSTRACT



### Funding

No funding was obtained for this study.

### Conflict of Interest

The authors have no financial conflicts of interest.

### Informed Consent

This type of study does not require informed consent.

### Ethics Approval

This research did not require ethical approval as it does not involve human subjects, their data, or biological samples.

## INTRODUCTION

Pedicle screws are the most fundamental and commonly used implants in spine fusion surgery.<sup>3,7,21</sup> The precise insertion of pedicle screws is crucial for the success of the fusion, and intraoperative C-arm X-rays are universally used for accurate pedicle screw placement due to their simplicity and relatively low cost.<sup>12,31</sup> However, the malposition rate is approximately 10%–40% and the use of intraoperative C-arm X-rays has also increased radiation exposure.<sup>13,20</sup> Several different modalities, such as navigation systems, have been developed for accurate insertion of the pedicle screw and reduction of radiation exposure.<sup>12,25,33</sup> Unlike C-arm X-rays, the computed tomography (CT)-based navigation system provides 3-dimensional images, demonstrating high accuracy in pedicle screw placement and is used in some advanced hospitals.<sup>29,30</sup> However, it has a steep learning curve, requires significant preoperative preparation time, and faces issues such as positional discrepancies between the navigation images and the actual patient.<sup>20,29</sup> To address these limitations, the intraoperative O-arm navigation system has been introduced, which does not require preoperative image preparation or repetitive intraoperative registration. This system has been reported to significantly increase the accuracy of pedicle screw placement.<sup>8,9,30</sup> Although the intraoperative O-arm navigation system greatly improves accuracy, its high cost limits its general use, so it is only used in a few hospitals.

There is increasing interest in the use of augmented reality systems in spine surgery as part of a practical free hand technique and as an alternative to current approaches such as C-arm X-ray and navigation systems.<sup>6,11,32</sup> The augmented reality system can project the patient's

anatomical structure directly onto the surgical field using images taken before surgery. However, to integrate external spine instruments into the augmented reality system, an additional recognition device is required. Combined with computer-assisted image guidance technology, deep learning technology is widely used in the spine field.<sup>2,4,5,19,26)</sup> In particular, the use of deep learning in pedicle screw insertion has also been reported. Esfandiari et al. provide a framework for automatic segmentation and posture estimation of pedicle screws using deep learning technology based on C-arm X-ray and, the calculated pose estimation accuracy was  $1.93^{\circ} \pm 0.64^{\circ}$  and  $1.92 \pm 0.55$  mm on clinically realistic X-rays.<sup>10)</sup> Therefore, in order to enhance the patient's surgical prognosis and compensate for the shortcomings of screw fixation, it is believed that technology that can be combined with imaging applications such as computer vision in the operating room is necessary. Meanwhile, the You Only Look Once (YOLO) model utilizes a fully convolutional neural network (CNN) to process the entire image at once.<sup>14,15)</sup> This network analyzes the image, divides it into a grid, and predicts bounding boxes and class probabilities for objects within each grid cell.<sup>14)</sup> YOLO has been successfully applied in the medical domain.<sup>1)</sup> It can be trained to detect and localize lesions in medical images, aiding in the diagnosis of diseases like pressure ulcers. It can also perform general object detection in medical images. Furthermore, an oriented bounding boxes (OBBs)-based YOLO model was used to recognize multiple surgical instrument tips.<sup>28)</sup> This model considers the center, angle, and other key information related to surgical instruments. Therefore, the purpose of this study is to develop a deep learning-based object detection model specialized for spine instruments to accurately recognize screws and localize and estimate their direction in augmented reality systems, and to investigate the feasibility of this model.

## MATERIALS AND METHODS

### Dataset

We collected 100 pedicle screw dataset images from brochures and website images provided by manufacturers (**SUPPLEMENTARY TABLE 1**) that provide pedicle screw systems used in spinal fusion (**TABLE 1**).

### Annotation and data augmentation

Following the initial data collection, the images underwent directional labeling and annotation using Roboflow annotation tool.<sup>16)</sup> Annotation processes ground truth information with class 0 as the pedicle screw and outputs predictions in the x, y, w, h, and r (xywhr) format. Here, this format represents the object's center point (x, y), width (w), height (h), and rotation angle (r). Subsequently, data augmentation techniques were employed to generate additional images, including variations in blur, brightness, and rotation. This process yielded a final dataset of 300 images, which was then segregated into training, validation, and test sets at the ratio of 70%:20%:10%, respectively.

**TABLE 1.** Characteristics of the original pedicle screw image sets used for modeling

Character	Original images (n)	%	Augmented images* (n)	%
Screw alone	43	43.00	121	40.33
Screw with assemble system	15	15.00	46	15.33
Screw with hand gloves	15	15.00	47	15.67
Screw with spine bone	11	11.00	38	12.67
Multiple screws	16	16.00	48	16.00
Total	100	100.00	300	100.00

\*Note: Blur, brightness, and rotation techniques are applied to original images.

**Model architecture**

For real-time detection of pedicle screws, YOLOv8 was used.<sup>14,16)</sup> The model consists of modules: head, bottle neck, and backbone. Backbone is a network main body that extracts features of images and improves object detection performance, and bottle neck module (C2f, faster implementation of the cross stage partial bottleneck with 2 convolutions module) is a key component that reduces feature channel dimensions while preserving spatial information and maintains model efficiency while extracting informative features. The head has an anchor-free structure that considers accuracy and efficiency, and is the part that generates the final output. The output from each detection head goes through a decoding process to generate detections with oriented bounding boxes and its classification using a sigmoid activation function, with binary cross entropy (BCE) loss measuring the difference between predicted and ground-truth class labels.<sup>22)</sup> And BCE measures the difference between the predicted class probabilities and the ground-truth labels (one-hot encoded) in equation 1.

$$BCE = -\sum [t(c) \times \log\{p(c)\} + \{1-t(c)\} \times \log\{1-p(c)\}] \quad (1)$$

where the predicted class probabilities  $p(c)$  and the ground-truth one-hot encoded labels  $t(c)$ ,  $c$  iterates over all class categories. The input images were resized to 640×640 pixels to match the model’s expectations. And normalization was applied to improve training stability. In YOLOv8’s backbone for the feature extraction, the five feature maps named p1, p2, p3, p4, and p5 represent the outputs at different stages of the convolutional layers (FIGURE 1). These stages progressively extract features of increasing complexity and abstraction. P1 and P2 (early layers) capture basic, low-level features like edges, corners, and simple shapes. They provide crucial foundational information for higher-level feature extraction. They capture global context, relationships between objects, and features that are essential for detecting larger or distant objects in the image. Meanwhile, by utilizing multiple feature maps from different stages (P3, P4, P5) in the detection head, YOLOv8 can predict bounding boxes for objects at different scales. The higher-resolution features (P3) are better suited for small or close objects, while the higher-level features (P4, P5) excel at detecting larger or distant objects.

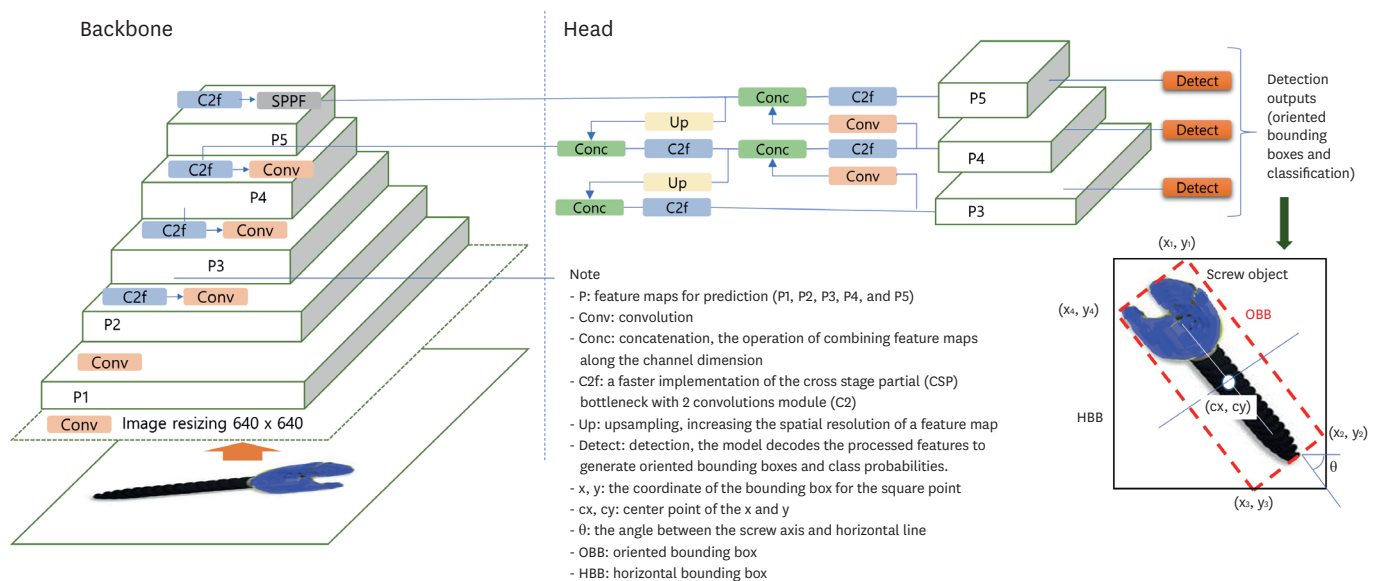


**FIGURE 1.** The model architecture of the YOLOv8-OB for this study. YOLO: You Only Look Once, OBB: oriented bounding box.

YOLOv8-OBB utilizes the corner points (obtained from handling the ground truth information for object detection or directly provided in the dataset) for internal training purposes.<sup>23)</sup> The model treats these points as the ground truth representation of the object during loss calculations and network optimization. While the model trains using corner points internally, it leverages the xywhr format for predicted outputs. The predicted x, y, w, h, and r values likely correspond to the estimated center point, width, height, and rotation of the detected object.

### External validation

To simulate a potential real-world application in an operating room equipped with a computer vision system, we employed a web camera for a preliminary test. In addition to internal testing of model training, external validation was conducted on three pedicle screws test images. And the model has detected the confidence score, which reflects its confidence in the prediction, along with the rotation angle for the images. A computer vision system employing the Logitech HD Webcam C270 (Logitech Inc., San Jose, CA, USA) was utilized to assess the potential for instrument localization within the operating room environment. The system detected and determined the direction of spine surgery instruments through image analysis from a web camera.

### Performance metrics

Loss in model training epochs, mAP50, and mAP50-95 in YOLO were evaluated to measure the performance of an object detection model. The mean average precision (mAP) was calculated for mAP50 and mAP50-95. The metric summarizes the overall precision (accuracy) of the model across all classes in your dataset. Meanwhile, intersection over union (IoU) is a metric used to measure the overlap between the predicted bounding box and the actual bounding box for the object, with a higher IoU indicating a better match between the prediction and the actual object. Again, the mAP50 is calculated at an IoU threshold of 0.5. It essentially measures how well the model performs in detecting objects with a 50% overlap between the predicted and ground truth bounding boxes. For the mAP50-95, this refers to the average mAP calculated across a range of IoU thresholds from 0.5 to 0.95. the mAP50-95 provides a more comprehensive picture of the model's performance by considering its ability to detect objects with varying degrees of overlap. And both the precision (how many detections were correct) and recall (how many actual objects were detected) of the model for that class were calculated for a particular class consideration.

### Programming environment

Python 3.10.12, PyTorch 2.2.1, i7, Intel® i9 processor, and NVIDIA® GeForce RTX™ 4060 were used to develop the YOLOv8-OBB model.

## RESULTS

### Pedicle screw orientation detection

As a result of performing training for 100 epochs using Adam optimizer through YOLOv8 OBB modeling, the prediction result for the test image is shown in **FIGURE 2**. The images of OBB prediction results corresponding to **FIGURE 2A-D** are **FIGURE 2E-H**. The model detects objects for screws in all test images, and recognizes objects in the direction of screw insertion or progress by outputting a bounding box in the direction of the screw rather than outputting a bounding box parallel to the image. The result was shown in **FIGURE 2E-H**.

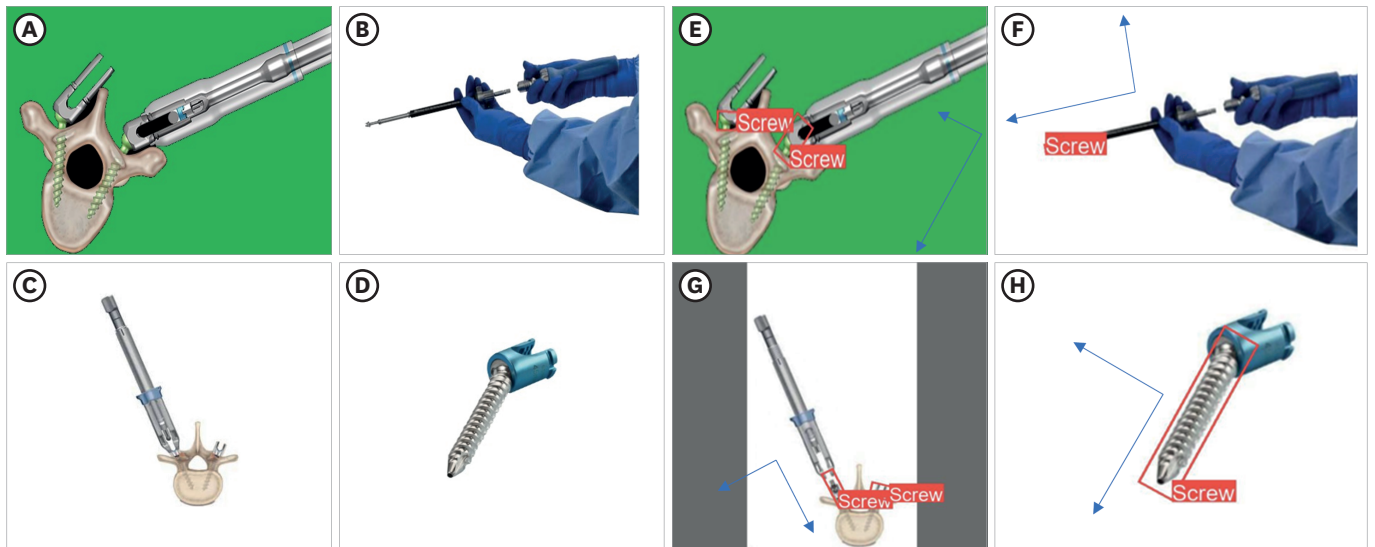


**FIGURE 2.** Test image sets and the prediction output images for the model of OBB. The images of OBB prediction results corresponding to A to D are E to H in FIGURE 2. The model not only detected objects for screws in all test images, but recognized objects for screw insertion and direction by outputting a bounding box for the direction of the screw. OBB: oriented bounding box.

### Prediction for the pedicle screw assembly

**FIGURE 3** shows the results predicted through the model developed through this study on screw assembly images. Real-world estimation result of pedicle screw for a maximum confidence score of 0.90 in the scene was detected in **FIGURE 3A**. Furthermore, the direction of the screw was detected and displayed as a bounding box, and the image position of the center coordinates (93, 522) and the orientation angle of 147.57 degrees were detected in **FIGURE 3B**. Localization information about the corner positions of the detected boxes was also calculated in the image or scene. The model achieved an average confidence score of  $0.66 \pm 0.28$  across the 3 test images for the predicted bounding boxes. The predicted rotation angles exhibited a mean of  $141.10^\circ \pm 22.95^\circ$ .

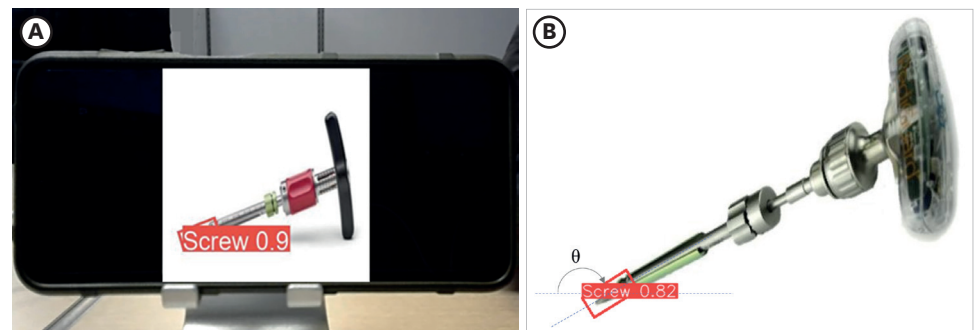


**FIGURE 3.** Prediction outcomes through the model developed through this study on screw assembly images. (A) Real-world estimation result of pedicle screw in the scene detection and prediction using web-camera (Logitech HD Webcam C270; Logitech Inc.). (B) Specific localization and detection results of the direction for the screw as a bounding box, and location of the center coordinates (93, 522) in the image or scene and the orientation angle of 147.57 degrees. Note: Confidence score of the detection: 0.82, Coordinates of the top-left (x1, y1) and bottom-right corners (x2, y2) of the OBB: (58.1528, 492.9121, 128.3769, 551.9011), Center coordinates (x, y), width (w), height (h) of the OBB: (93.2648, 522.4066, 65.0638, 28.5457), and Rotation angle ( $\theta$ ): 147.57 degrees. OBB: oriented bounding box.



**Model performance metrics**

For pedicle screw detection of the model, classification and distribution focal loss through detection of bounding box, screw and non-screw parts were calculated from 1 epoch to 100 epochs (FIGURE 4A). Where the distribution focal loss is a variant of the focal loss function designed for imbalanced datasets, common in object detection. Damping exists, but stabilized after 90 epochs. FIGURE 4B is the result of calculating mAP50 and mAP50-95. The precision of mAP50 showed a maximum of 0.83 at 93 epochs. And, the precision of mAP50-95 converged at over 0.5 (FIGURE 4B). Performance indicators for the model's F1 score, precision, and recall were calculated in TABLE 2. The F1-score was 0.86, precision 1.00, recall 0.80, mAP50max 0.83, and mAP50-95max 0.56.

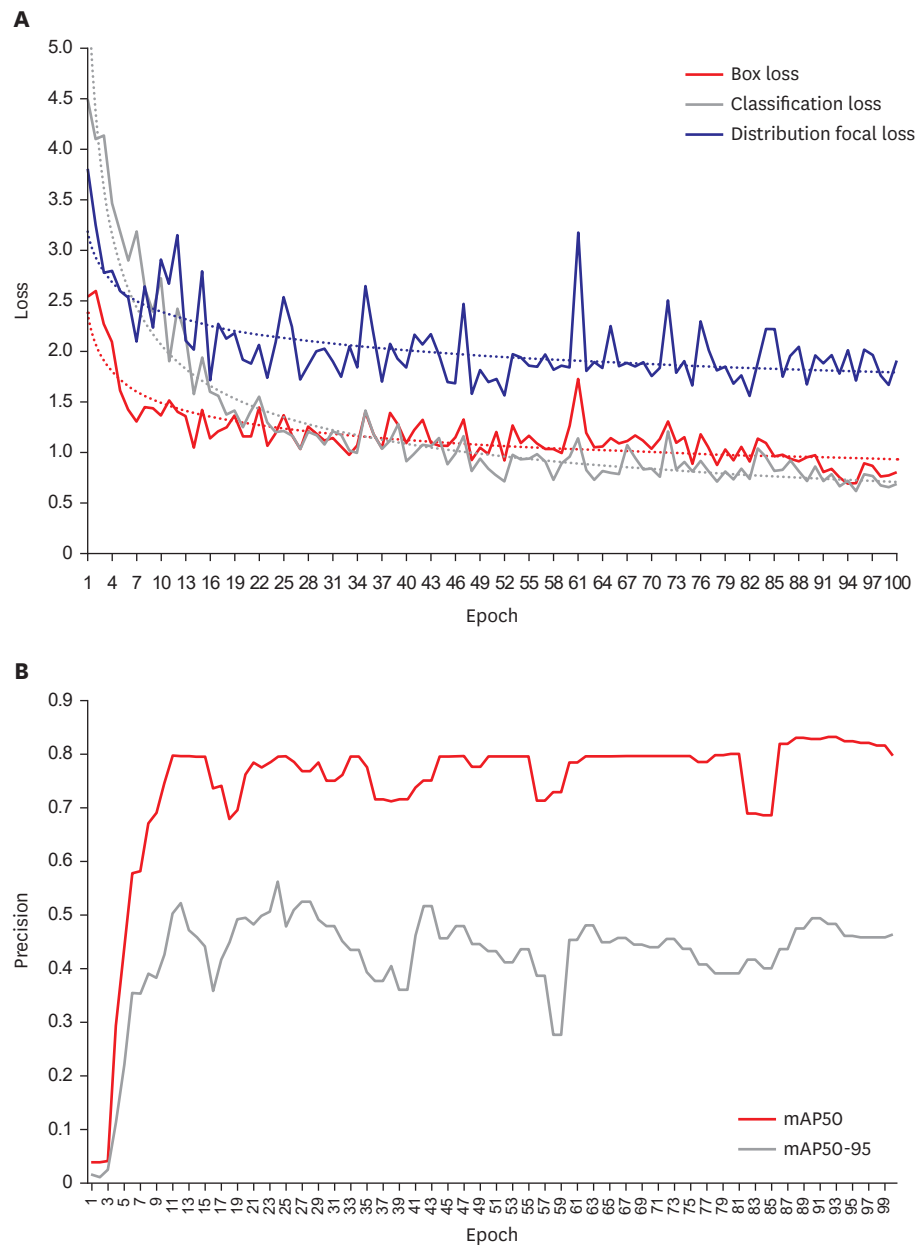


**FIGURE 4.** The box, classification, and distribution focal loss in training by 100 epochs (A) and the mAP calculated at an IoU threshold of 0.5 and 0.5 to 0.95 (B). mAP: mean average precision.

**TABLE 2.** The performance metrics for F1-score, precision, recall, mAP50, and mAP50-95 of the model

Metrics	F1-score	Precision	Recall	mAP50	mAP50-95
Value	0.86	1.00	0.80	0.83	0.56
Condition	Confidence level* 0.40	Confidence level* 0.43	mAP50	Max	Max

mAP: mean average precision.

\*Note: Confidence level is the classification probability for the pedicle screw detection.

## DISCUSSION

### Oriented bounding boxes for pedicle screws

We detected the surgical tool along the direction of the screw object, rather than through a simple bounding box horizontal to the image (**FIGURE 2**). In the image collection process for the pedicle screw, we tried to collect images considering the complex screw characteristics as shown in **TABLE 1**. However, in an actual operating room environment, when the screw retraction process is not well recognized through computer vision while the operator is handling the assembly, a challenge arises in which the region of interest detection area is reduced (**FIGURE 2A-C**). In this case, there is a need for an algorithm that subdivides detection features into an enlarged area, or the need to add trajectory necessary for direction detection. In order to accurately localize the pedicle screw in this study, we calculated detailed information about the center point coordinates, and direction angle of the detection area for prediction outcome of the surgical instrument (**FIGURE 3**). Localization of surgical instruments in computer vision is crucial for several reasons. Firstly, it allows for a more complete understanding of the surgical scene, similar to how object detection helps understand a general image. By knowing the exact location of each instrument, the computer can build a more comprehensive picture of the operative field. Secondly, precise localization is vital for tasks like instrument tracking and surgical navigation. This empowers computer-assisted or robotic surgery systems to precisely track instrument movement, ensuring smooth and safe manipulation within the delicate surgical environment. Finally, accurate localization can be used for tasks like anomaly detection. If a specific instrument is unexpectedly missing from its expected location, the system can raise an alarm, potentially preventing errors or delays during surgery. Overall, localization underpins various functionalities in computer vision for surgical applications, leading to a safer, more efficient, and potentially less invasive surgical experience.<sup>18,19,27)</sup>

### Clinical application of the pedicle screw detection

A deep learning model trained on a dataset of CT scans of patients with spinal diseases can analyze the patient's spinal anatomy.<sup>10)</sup> The model can identify key features such as vertebrae, pedicles, and potential nerve pathways. Models generated through methods such as those in this study can predict the optimal entry point, trajectory, and depth of each pedicle screw.<sup>10)</sup> This prediction may consider factors such as bone density, screw size, and potential risk of nerve impingement. Meanwhile, deep learning can analyze complex anatomical details, potentially making screw placement more accurate and reducing the risk of complications. Fluoroscopy (real-time X-rays) is currently used to guide screw placement, but both surgeon and patient are exposed to radiation. Computer vision technology using deep learning is still in development as a follow-up study, but research is ongoing to improve deep learning models and optimize surgical computer system integration.<sup>2,28)</sup> Deep learning models can be further personalized by considering the anatomy and medical history of individual patients. Additional imaging techniques, such as fluoroscopy or CT scans, can be used to analyze screw placement during surgery in real time, and an image-guided computer vision system



can provide surgeons with feedback to avoid critical structures during surgical approaches.<sup>4,5)</sup> Although there are challenges to overcome, the combination of deep learning and augmented reality has the potential to significantly improve the safety, accuracy, and efficiency of spine surgery, especially pedicle screw placement. And detecting and recognizing surgical instruments is crucial for efficient surgery. Researchers have explored deep learning techniques for surgical tool detection, including CNNs.<sup>24)</sup> These methods can enhance robotic surgery, instrument tracking, and training.

### Accuracy and speed for modeling of YOLOv8

In object detection deep learning models, anchor boxes are essentially a set of predefined boxes in various sizes and shapes that are placed on a grid system over the input image.<sup>15)</sup> The model then refines these anchor boxes to predict the actual bounding boxes of objects in the image. First, instead of predicting bounding boxes from scratch for every single location in the image, anchor boxes provide a good starting point, making the process more efficient.<sup>17)</sup> Second, by using a variety of anchor box sizes, the model can handle objects of different scales within the image. YOLOv8 which is employed in this study, has maintained that the anchor-free design offers a good balance between accuracy and speed. The model utilizes an anchor-free object detection method.<sup>14)</sup> YOLOv8 directly predicts the bounding box coordinates (center point, width, and height) relative to a grid cell in the image. This approach offers more flexibility in detecting objects of varying sizes and aspect ratios without needing a predefined set of anchors. However, conventional Models (YOLOv1-v7) on predefined anchor boxes of various sizes and aspect ratios. The model predicts offsets and adjustments to these anchor boxes to get the final bounding boxes for objects. Another discussion thread explores the possibility of a hybrid approach where YOLOv8 might utilize a small set of learned anchor boxes along with its current architecture.<sup>14)</sup> This could potentially improve detection accuracy for certain object classes or specific aspect ratios. The anchor-free design simplifies the model architecture and potentially reduces training complexity. However, some researchers are exploring if there might be trade-offs in terms of inference speed compared to anchor-based models.<sup>28)</sup>

### Considering the complex operating room environment

We produced efficient modeling results using 100 image sets (**TABLE 1, FIGURE 1**). In this study, 300 expanded images with blurring, rotation, and brightness adjusted considering data augmentation were used. In future studies, image collection in a complex operating room environment is necessary. By training the model using images, directional detection can be performed in more complex environments. Additionally, by employing screw image data from a wider variety of manufacturers, it is possible to detect the directionality of surgical instruments for computer-based spine surgery. To complement our internal model training evaluation, we performed external validation using three test images containing pedicle screws (**FIGURE 3**). Future work should involve expanding the external validation process by analyzing detection results on a significantly larger dataset of test images. While this study focused on the detection and orientation of surgical instruments within the operating scene, future investigations could explore the potential of segmentation models. These models might be capable of simultaneously recognizing not only surgical instruments but also the surgeon's hands and the patient's spinal vertebrae, offering a more comprehensive analysis of the surgical scene.

## CONCLUSION

In this study, we investigated the application of a deep learning-based object detection model for accurate localization and orientation estimation of intraoperative spinal fixation instruments for computer-based spine surgery. Although the model was not trained through image collection in a complex operating room environment and the number of screw image data was limited, the possibility of detecting the directionality of surgical instruments for computer-based spine surgery was confirmed.

## SUPPLEMENTARY MATERIAL

### SUPPLEMENTARY TABLE 1

List of manufacturers and corresponding product names for the pedicle screw image sets used in the study

## REFERENCES

1. Aldughayfiq B, Ashfaq F, Jhanjhi NZ, Humayun M. YOLO-based deep learning model for pressure ulcer detection and classification. *Healthcare (Basel)* **11**:1222, 2023 [PUBMED](#) | [CROSSREF](#)
2. Amiot LP, Labelle H, DeGuise JA, Sati M, Brodeur P, Rivard CH. Computer-assisted pedicle screw fixation. A feasibility study. *Spine (Phila Pa 1976)* **20**:1208-1212, 1995 [PUBMED](#) | [CROSSREF](#)
3. Barrey CY, Ponnappan RK, Song J, Vaccaro AR. Biomechanical evaluation of pedicle screw-based dynamic stabilization devices for the lumbar spine: a systematic review. *SAS J* **2**:159-170, 2008 [PUBMED](#) | [CROSSREF](#)
4. Benzakour A, Altsitzioglou P, Lemée JM, Ahmad A, Mavrogenis AF, Benzakour T. Artificial intelligence in spine surgery. *Int Orthop* **47**:457-465, 2023 [PUBMED](#) | [CROSSREF](#)
5. Burström G, Buerger C, Hoppenbrouwers J, Nachabe R, Lorenz C, Babic D, et al. Machine learning for automated 3-dimensional segmentation of the spine and suggested placement of pedicle screws based on intraoperative cone-beam computer tomography. *J Neurosurg Spine* **31**:147-154, 2019 [PUBMED](#) | [CROSSREF](#)
6. Burström G, Persson O, Edström E, Elmi-Terander A. Augmented reality navigation in spine surgery: a systematic review. *Acta Neurochir (Wien)* **163**:843-852, 2021 [PUBMED](#) | [CROSSREF](#)
7. Cabrera JP, Camino-Willhuber G, Muthu S, Guiroy A, Valacco M, Pola E. Percutaneous versus open pedicle screw fixation for pyogenic spondylodiscitis of the thoracic and lumbar spine: systematic review and meta-analysis. *Clin Spine Surg* **36**:24-33, 2023 [PUBMED](#) | [CROSSREF](#)
8. Costa F, Cardia A, Ortolina A, Fabio G, Zerbi A, Fornari M. Spinal navigation: standard preoperative versus intraoperative computed tomography data set acquisition for computer-guidance system: radiological and clinical study in 100 consecutive patients. *Spine (Phila Pa 1976)* **36**:2094-2098, 2011 [PUBMED](#) | [CROSSREF](#)
9. Cui G, Wang Y, Kao TH, Zhang Y, Liu Z, Liu B, et al. Application of intraoperative computed tomography with or without navigation system in surgical correction of spinal deformity: a preliminary result of 59 consecutive human cases. *Spine (Phila Pa 1976)* **37**:891-900, 2012 [PUBMED](#) | [CROSSREF](#)
10. Esfandiari H, Newell R, Anglin C, Street J, Hodgson AJ. A deep learning framework for segmentation and pose estimation of pedicle screw implants based on C-arm fluoroscopy. *Int J CARS* **13**:1269-1282, 2018 [PUBMED](#) | [CROSSREF](#)
11. Felix B, Kalatar SB, Moatz B, Hofstetter C, Karsy M, Parr R, et al. Augmented reality spine surgery navigation: increasing pedicle screw insertion accuracy for both open and minimally invasive spine surgeries. *Spine (Phila Pa 1976)* **47**:865-872, 2022 [PUBMED](#) | [CROSSREF](#)
12. Feng W, Wang W, Chen S, Wu K, Wang H. O-arm navigation versus C-arm guidance for pedicle screw placement in spine surgery: a systematic review and meta-analysis. *Int Orthop* **44**:919-926, 2020 [PUBMED](#) | [CROSSREF](#)
13. Gebhard F, Kraus M, Schneider E, Arand M, Kinzl L, Hebecker A, et al. Radiation dosage in orthopedics -- a comparison of computer-assisted procedures. *Unfallchirurg* **106**:492-497, 2003 [PUBMED](#) | [CROSSREF](#)

14. Hussain M. YOLO-v1 to YOLO-v8, the rise of YOLO and its complementary nature toward digital manufacturing and industrial defect detection. *Machines* **11**:677, 2023 [CROSSREF](#)
15. Jiang P, Ergu D, Liu F, Cai Y, Ma B. A review of YOLO algorithm developments. *Procedia Comput Sci* **199**:1066-1073, 2022 [CROSSREF](#)
16. Jocher G, Chaurasia A, Qiu J. Yolo by ultralytics [Computer Software]. 2023
17. Ju RY, Cai W. Fracture detection in pediatric wrist trauma X-ray images using YOLOv8 algorithm. *Sci Rep* **13**:20077, 2023 [PUBMED](#) | [CROSSREF](#)
18. Laina I, Rieke N, Rupprecht C, Vizcaíno JP, Eslami A, Tombari F, et al. Concurrent segmentation and localization for tracking of surgical instruments in Descoteaux M, Maier-Hein L, Franz A, Jannin P, Collins DL, Duchesne S (eds): *Medical Image Computing and Computer-Assisted Intervention – MICCAI 2017: 20th International Conference, Quebec City, QC, Canada, September 11-13, 2017, Proceedings, Part II*. Cham, pp664-672, 2017
19. Lavallée S, Sautot P, Troccaz J, Cinquin P, Merloz P. Computer-assisted spine surgery: a technique for accurate transpedicular screw fixation using CT data and a 3-D optical localizer. *J Image Guid Surg* **1**:65-73, 1995 [PUBMED](#) | [CROSSREF](#)
20. Lee MH, Lin MH, Weng HH, Cheng WC, Tsai YH, Wang TC, et al. Feasibility of intra-operative computed tomography navigation system for pedicle screw insertion of the thoraco-lumbar spine. *J Spinal Disord Tech* **26**:E183-E187, 2013 [PUBMED](#) | [CROSSREF](#)
21. Linhares D, Neves N, Ribeiro da Silva M, Almeida Fonseca J. Analysis of the Cochrane Review: Pedicle Screw Fixation for Traumatic Fractures of the Thoracic and Lumbar Spine. *Cochrane Database Syst Rev*. 2013;**05**:CD009073. *Acta Med Port* **29**:297-300, 2016 [PUBMED](#) | [CROSSREF](#)
22. Liu Z, Wang S. Broken corn detection based on an adjusted YOLO with focal loss. *IEEE Access* **7**:68281-68289, 2019 [CROSSREF](#)
23. Peng J, Chen Q, Kang L, Jie H, Han Y. Autonomous recognition of multiple surgical instruments tips based on arrow OBB-YOLO network. *IEEE Trans Instrum Meas* **71**:1-13, 2022 [CROSSREF](#)
24. Rodrigues M, Mayo M, Patros P. Surgical tool datasets for machine learning research: a survey. *Int J Comput Vis* **130**:2222-2248, 2022 [CROSSREF](#)
25. Shin MH, Ryu KS, Park CK. Accuracy and safety in pedicle screw placement in the thoracic and lumbar spines : comparison study between conventional C-arm fluoroscopy and navigation coupled with O-arm® guided methods. *J Korean Neurosurg Soc* **52**:204-209, 2012 [PUBMED](#) | [CROSSREF](#)
26. Smith HE, Welsch MD, Sasso RC, Vaccaro AR. Comparison of radiation exposure in lumbar pedicle screw placement with fluoroscopy vs computer-assisted image guidance with intraoperative three-dimensional imaging. *J Spinal Cord Med* **31**:532-537, 2008 [PUBMED](#) | [CROSSREF](#)
27. Sommer F, Goldberg JL, McGrath L Jr, Kirnaz S, Medary B, Härtl R. Image guidance in spinal surgery: a critical appraisal and future directions. *Int J Spine Surg* **15**:S74-S86, 2021 [PUBMED](#) | [CROSSREF](#)
28. Terven J, Córdova-Esparza DM, Romero-González JA. A comprehensive review of YOLO architectures in computer vision: from YOLOv1 to YOLOv8 and YOLO-NAS. *Mach Learn Knowl Extr* **5**:1680-1716, 2023 [CROSSREF](#)
29. Tian NF, Xu HZ. Image-guided pedicle screw insertion accuracy: a meta-analysis. *Int Orthop* **33**:895-903, 2009 [PUBMED](#) | [CROSSREF](#)
30. Tormenti MJ, Kostov DB, Gardner PA, Kanter AS, Spiro RM, Okonkwo DO. Intraoperative computed tomography image-guided navigation for posterior thoracolumbar spinal instrumentation in spinal deformity surgery. *Neurosurg Focus* **28**:E11, 2010 [PUBMED](#) | [CROSSREF](#)
31. Tumbiolo S, Gerardi RM, Brunasso L, Costanzo R, Lombardo MC, Porcaro S, et al. Pedicle screw placement aided by C-arm fluoroscopy: a “nevermore without” technology to pursue optimal spine fixation. *Acta Neurochir Suppl (Wien)* **135**:213-217, 2023 [PUBMED](#) | [CROSSREF](#)
32. Yamout T, Orosz LD, Good CR, Jazini E, Allen B, Gum JL. Technological advances in spine surgery: navigation, robotics, and augmented reality. *Orthop Clin North Am* **54**:237-246, 2023 [PUBMED](#) | [CROSSREF](#)
33. Yao Y, Jiang X, Wei T, Yao Z, Wu B, Xu F, et al. A real-time 3D electromagnetic navigation system for percutaneous pedicle screw fixation in traumatic thoraco-lumbar fractures: implications for efficiency, fluoroscopic time, and accuracy compared with those of conventional fluoroscopic guidance. *Eur Spine J* **31**:46-55, 2022 [PUBMED](#) | [CROSSREF](#)